NF-GNN: Network Flow Graph Neural Networks for Malware Detection and Classification *

Julian Busch¹, Anton Kocheturov², Volker Tresp^{1,3}, and Thomas Seidl¹

Ludwig-Maximilians-Universität München, Munich, Germany {busch, seidl}@dbs.ifi.lmu.de
Siemens Technology, Princeton, NJ, USA anton.kocheturov@siemens.com
Siemens AG, Munich, Germany volker.tresp@siemens.com

Abstract. Malicious software (malware) poses an increasing threat to the security of communication systems, as the number of interconnected mobile devices increases exponentially. While some existing malware detection and classification approaches successfully leverage network traffic data, they treat network flows between pairs of endpoints independently and thus fail to leverage the rich structural dependencies in the complete network. Our approach first extracts flow graphs and subsequently classifies them using a novel graph neural network model. We present three variants of our base model, which all support malware detection and classification in supervised and unsupervised settings. We evaluate our approach on flow graphs that we extract from a recently published dataset for mobile malware detection that addresses several issues with previously available datasets. Experiments on four different prediction tasks consistently demonstrate the advantages of our approach and show that our graph neural network model can boost detection performance by a significant margin.

Keywords: Malware Detection · Graph Neural Networks

1 Introduction

Malicious software (malware) poses a major threat to the security of information technology (IT) and operational technology (OT) in private and corporate environments. Along with an increasing degree of digitalization and the rise of new technologies such as the Internet of Things (IoT), an increasing number of devices including mobile devices, such as smartphones, and Industrial Control Systems (ICS), become connected and thus are potential targets for attacks. Accurate detection and classification of malware is thus a vital task to ensure the security of such systems.

^{*} This work was done during an internship at CT RDA BAM IBI-US, Siemens Technology, Princeton, NJ, USA.

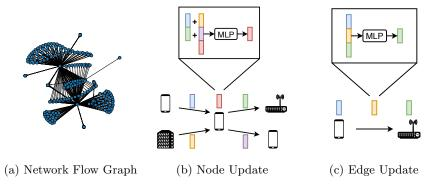


Fig. 1: Directed network flow graph extracted from network traffic generated during execution of the Scareware FakeAV (1a). Not shown: edge feature vectors. By sequentially updating node (1b) and edge feature vectors (1c) by neural message passing, our model learns how devices communicate with each other.

In this work, we focus on dynamic malware detection and classification. In contrast to static methods, which analyze a candidate application's source code or the structure of its executable, dynamic methods execute the application in a controlled environment and analyze dynamic behavior that can usually not be extrapolated from static data. More specifically, we consider network traffic data generated during execution of the application, which provides valuable insights about the dynamic and potentially malicious behavior affecting that application. However, in contrast to existing works, which classify individual network flows between two endpoints, i.e., the aggregated communication between the two endpoints during some time frame, we construct a communication graph from all recorded network flows between any two endpoints during that time frame to obtain a rich representation of communication in the network. To the best of our knowledge, no existing work has considered this setting so far. While classical machine learning methods have proven successful for malware detection and classification [12], deep learning approaches have not been studied as extensively. Deep learning methods offer an additional advantage of being able to automatically learn suitable feature representations of the input data optimized for the task at hand, in contrast to traditional feature engineering approaches. Our novel graph neural network model is able to learn suitable representations from extracted network flow graphs. Along with a base model for representation learning, we propose three derived model variants, a graph classifier, a graph autoencoder and a one-class graph neural network, which are able to perform supervised malware detection and classification and unsupervised malware detection, respectively.

We evaluate our approach on a graph dataset extracted from network flow features obtained from traffic generated by android applications executed on real mobile devices. The original flow features are provided by [23]. The data

was collected in a carefully designed environment to account for several common defects observed in previously used datasets. Instead of classifying individual network flows, as the original work proposes, we follow our graph-based approach and construct a flow graph for each execution of a candidate application. Experiments on four different prediction tasks, supervised binary, category and family classification, and unsupervised detection, consistently demonstrate the significantly superior detection performance of our approach. Our neural network model additionally boosts performance compared to baseline models, even in settings with unlabeled data and small amounts of available training data.

2 Related Work

A comprehensive overview over existing machine learning methods for malware detection and classification is provided by a recent survey [12]. Methods relying on network traffic data mainly differ by which specific features are extracted and which machine learning algorithm is used. To the best of our knowledge, all existing approaches focus on classifying individual network traffic between two endpoints in a network, possibly at different resolutions. For instance, [5] describes different resolution levels, ranging from single transactions over flows to conversations aggregating multiple flows between two endpoints over a duration of time.

Existing methods typically report high performance on datasets which exhibit various common defects. A recently published dataset [23] has addresses these issues by providing a sufficient number of malware samples from diverse malware categories and families with a realistic distribution of benign and malicious applications. Additionally, each application is executed on an actual physical device instead of an emulator or a virtual machine to accurately capture its actual behavior. Instead of classifying network flows individually as proposed by the authors, we instead extract network flow graphs from the given network traffic features. The results reported in [23] have been improved by adding new dynamic API-call features and combining a dynamic prediction model with a static prediction model [31] and by predicting labels for conversations instead of individual flows [1].

Existing graph-based approaches to malware detection and classification mostly focus on static analysis, considering function call graphs [20,15,17] or control graphs [11,4]. Dynamic graph-based approaches include [2], where graphs are constructed from instruction traces collected during execution, and [19], where system call graphs are considered. To the best of our knowledge, no existing work has considered graph-based approaches based on dynamically generated network traffic data. Deep learning methods have not been investigated as extensively as classical machine learning methods for network traffic-based approaches. Existing methods consider detection of endpoints generating malicious traffic [26] or intrusion detection [25]. To the best of our knowledge, no existing deep learning-based malware detection and classification method considers network flow graphs.

J. Busch et al.

While our proposed approach includes a novel graph neural network model for malware detection and classification, it could be more generally employed to solve other graph classification and graph anomaly detection tasks. While graph neural networks [6,13,3] have become a de-facto standard for machine learning problems on graph data, most existing models consider only node attributes, whereas our model focuses on edge attributes instead. Some existing models consider edge attributes [30,21,28,14,18,33], but none of these models is directly applicable to our setting, since they either consider multi-relational graphs or additionally focus on node attributes. Other existing models [29,35,24] focus on more specific tasks which differ from our setting.

3 Extraction of Network Flow Graph

To decide whether a particular candidate application is malicious, we collect all network traffic generated during execution of that application within a given time interval after installation. The resulting data consists of a set of network flows described by feature vectors which can be extracted from pcap-files using tools such as CICFlowMeter [10]. Each flow F describes network traffic between two endpoints during some time frame and has a feature vector $f \in \mathbb{R}^d$ attached to it. Typical features include the total number of bytes sent, mean and standard deviation of packet length, or minimum and maximum inter-arrival time of packets.

From the resulting set of flows \mathcal{F} , we extract a flow graph, where the nodes correspond to endpoints in the network and edges model communication between these endpoints. Instead of considering (IP, Port)-tuples, we factor out the port information and consider IP-endpoints for two main reasons: (1) Apart from standard ports, port selection is often arbitrary and would result in arbitrary and potentially misleading graph structure. (2) Empirically, we found (IP, Port)graphs to be very sparse and rather uninformative. In comparison, IP-graphs exhibit much more interesting structure. Figure 1 shows an exemplary graph extracted from real data. More specifically, for a set of flows \mathcal{F} , we extract a directed graph G = (V, E) where the nodes correspond to endpoints involved in any flow in \mathcal{F} and a directed edge is added for all pairs (s_i, t_i) for which there exists a flow F_i with source and target IP s_i and t_i , respectively. The feature vector assigned to this edge aggregates the features vectors $f_i \in \mathbb{R}^d$ of all flows F_i along this edge using the mean, median, standard deviation, skew and kurtosis functions and concatenating the aggregate values, resulting in a 5d-dim. feature vector for each edge.

Intuitively, the resulting graph captures how network traffic flows between different endpoints in the monitored network during a specific time frame. The graph structure reveals where traffic is flowing and the additional edge attributes describe how it is flowing. Connecting individual flows in a graph provides a much richer relational representation compared to treating flows individually. Thus, we expect models learning from these graphs to perform significantly better at

detection and classification tasks than models which classify individual flows. Our experimental results confirm this intuition.

4 Network Flow Graph Neural Networks

Formally, we are given a set of graphs $\mathcal{G} = \{G_1, \dots, G_N\}$, a set of edge feature matrices $X_i \in \mathbb{R}^{m_i \times d}$, $i = 1, \dots, N$, where $m_i = |E_i|$, and a label matrix $\hat{Y} \in \{0,1\}^{N \times c}$, where c is the number of classes. In a supervised anomaly detection setting, class labels could be binary (normal vs. anomalous) or multi-class (normal class and different categories or families of anomalies). For supervised classification, a labeled training data-set is given as described above and the task is to train a model which accurately predicts labels for new graphs not seen by the model during training. For unsupervised anomaly detection, the training set is not labeled and consists of normal data and (usually a relatively small fraction of) anomalous data. The model is required to learn a concept of normality from the training data and to correctly classify new graphs as either being normal or anomalous.

4.1 Learning Representations of Network Flow Graphs

Each input instance for our model is a directed graph G = (V, E) with edge feature matrix $X \in \mathbb{R}^{m \times d}$, where m := |E|. The representation learning part of our model computes latent representations of the edges and nodes in the graph and finally outputs a latent feature vector $h^{(1)} \in \mathbb{R}^h$ for each node in the graph. Such a vector intuitively describes how the corresponding endpoint interacts with other endpoints in the network. Depending on the availability of labels, variants of our model compute either predictions or an anomaly score for an input graph from its latent node feature vectors. The model is trained end-to-end such that the latent representations are optimized towards the specific task. The computational steps performed by our model can be summarized as follows:

$$E^{(0)} = f_1(X) \qquad \in \mathbb{R}^{m \times h} \tag{1}$$

$$H^{(0)} = f_2\left(\left[\hat{\mathbf{B}}_{in} E^{(0)}, \hat{\mathbf{B}}_{out} E^{(0)}\right]\right) \qquad \in \mathbb{R}^{n \times h}$$
 (2)

$$E^{(1)} = f_3 \left(\left[\hat{\mathbf{B}}_{in}^T H^{(0)}, \hat{\hat{\mathbf{B}}}_{out}^T H^{(0)}, E^{(0)} \right] \right) \in \mathbb{R}^{m \times h}$$
 (3)

$$H^{(1)} = f_4\left(\left[\hat{\hat{\mathbf{B}}}_{in} E^{(1)}, \hat{\hat{\mathbf{B}}}_{out} E^{(1)}, H^{(0)}\right]\right) \in \mathbb{R}^{n \times h}, \tag{4}$$

where $[\cdot, \cdot]$ denotes concatenation and f_1, \ldots, f_4 are Multi-Layer Perceptrons (MLPs) with appropriate input and output dimensions. As per default, we use single-layer MLPs $f_i(X) = q(XW_i + b_i)$ where W_i and b_i are the learnable parameters of the model and q is a non-linear activation. We further use ReLU activations and add batch normalization. The propagation matrices $\hat{B}_{in}, \hat{B}_{out} \in$

 $\mathbb{R}^{n \times m}$ are obtained from the node-edge incidence matrices B_{in} , $B_{out} \in \{0,1\}^{n \times m}$, indicating in- and out-going edges for each node, by substituting non-zero entries with normalized edge weights. Normalization is applied to preserve the scale of the feature vectors. In particular, we apply symmetric normalization as in [22]. Self-loops added for normalization are removed again such that the graph structure remains unchanged.

Illustrations of the performed node and edge feature updates are provided in Figure 1b and 1c, respectively. The first network layer (Equation 1-2) learns how endpoints interact with each other directly. Notably, incoming and outgoing traffic are modeled separately for each node. The optional second layer (Equation 3-4) additionally enables the model to learn how endpoints communicate indirectly with their 2-hop neighbors. Skip-connected node and edge features from the first layer give this layer direct access to previously learned features and aid in optimization [16,34]. In principle, one could add more layers to the model in a similar fashion to model interaction between more distant endpoints. However, the graphs considered usually have a relatively small diameter and in our experiments we observed best performance with either one or two layers.

4.2 Network Flow Graph Classifier

For supervised graph classification, we append two more layers to the representation learning module. First, a pooling layer aggregates all node feature vectors in the input graph to a single vector describing the whole graph. The second layer predicts the graph label from the pooled graph representation,

$$h = \operatorname{pool}\left(H^{(1)}\right) \qquad \in \mathbb{R}^h \tag{5}$$

$$y = \operatorname{softmax}(Wh + b) \qquad \in \mathbb{R}^{c}. \tag{6}$$

Above, pool denotes a pooling function, such as element-wise mean or maximum, which aggregates all node representations into a single embedding vector for the whole graph. Predictions are computed by a dense prediction layer. The model parameters are then optimized w.r.t. the *cross-entropy* loss. We denote this model as *NF-GNN-CLF*.

4.3 Network Flow Graph Autoencoder

For unsupervised anomaly detection, autoencoder models have been reported to perform well in practice [9]. In general, an autoencoder consists of two neural network modules. While an encoder learns compact and expressive representations of the model inputs, a decoder is supposed to reconstruct the original inputs from their learned representations. If the model is trained with exclusively or mostly normal data, the reconstruction loss can be interpreted as an anomaly score, where instances incurring a larger reconstruction loss are considered more anomalous. We propose a graph autoencoder model where our representation learning module acts as an encoder. The latent node representations $H^{(1)}$ are

then used to reconstruct the original edge feature vectors of the graph using a decoder, which is a mirrored version of the encoder:

$$E^{(2)} = f_5 \left(\left[\hat{\tilde{B}}_{in}^T H^{(1)}, \hat{\tilde{B}}_{out}^T H^{(1)} \right] \right) \in \mathbb{R}^{m \times h}$$
 (7)

$$H^{(2)} = f_6\left(\left[\hat{\tilde{B}}_{in} E^{(2)}, \hat{\tilde{B}}_{out} E^{(2)}, H^{(1)}\right]\right) \in \mathbb{R}^{n \times h}$$
 (8)

$$E^{(3)} = f_7 \left(\left[\hat{\tilde{B}}_{in}^T H^{(2)}, \hat{\tilde{B}}_{out}^T H^{(2)}, E^{(2)} \right] \right) \in \mathbb{R}^{m \times h}$$
 (9)

$$E^{(4)} = f_8 \left(E^{(3)} \right) \qquad \in \mathbb{R}^{m \times h} \tag{10}$$

If the encoder uses only a single layer, the first layer of the decoder (Equation 7–8) is dropped and the node embeddings $H^{(0)}$ are used as input instead. The model parameters are optimized w.r.t. a reconstruction loss

$$\mathcal{L}_{AE}(\mathcal{G}) = \frac{1}{N} \sum_{G_i \in \mathcal{G}} \frac{1}{m_i} \left\| X_i - E_i^{(4)} \right\|_F^2, \tag{11}$$

where $||\cdot||_F$ denotes the Frobenius norm. A similar loss was used in [8] to reconstruct node attributes, whereas our model operates on edge-attributed graphs. We denote this variant of our model as NF-GNN-AE.

4.4 One-Class Network Flow Graph Neural Network

Though autoencoder models perform well in practice, they don't optimize an anomaly detection objective directly. Deep SVDD [27] combines Support Vector Data Description (SVDD) [32] with a neural network for anomaly detection in a learned latent space. The main idea is to learn a transformation into a latent space such that most instances are mapped into a hypershere in that space and anomalous instances will fall outside of the hypersphere. We propose a one-class graph neural network consisting of our representation learning module and an additional pooling layer which summarizes each input graph into a single feature vector, similarly as for the supervised graph classifier. The model parameters are optimized w.r.t. a one-class loss [27]

$$\mathcal{L}_{OC}(\mathcal{G}) = \frac{1}{N} \sum_{G_i \in \mathcal{G}} \|h_i - \mu\|_2^2 + \frac{\lambda}{2} \sum_{i=1}^4 \|W_i\|_F^2,$$
 (12)

where $\mu \in \mathbb{R}^h$ denotes the center of the hyper-sphere in latent space. The center is initialized with the mean embedding vector of all graphs in \mathcal{G} after the first forward-pass and does not change thereafter. The second part of the loss regularizes the model parameters to limit model complexity. Bias vectors have been removed from all layers to prevent trivial solutions [27]. We denote this variant of our model as NF-GNN-OC.

5 Experiments

We evaluate our approach on a graph dataset we extract from the network traffic data collected by [23]. The dataset consists of 2126 samples, where each sample corresponds to one instance of an android application installed and executed on a mobile phone. For each sample, all network flows appearing in the network during execution are captured. For each flow, 80 features are recorded. For more detailed information about data collection, we refer to [23]. For each sample, 3 different labels are available, a binary label indicating whether the application is malicious or not, a category label with 5 possible values indicating the general class of malware, and a family label with 36 different values indicating the specific type of malware. Malware families with fewer than 9 samples have been removed to ensure a reasonable split into train, validation and test sets. Consequently, for the family prediction task, only 2071 samples are available.

We extract a graph for each sample as described in Section 3 and remove the flow id, timestamp, and endpoint IP and port information from the feature set. Additionally, we remove all features that are constant among all edges of all graphs, leaving 330 edge features. To be able to compare against baselines apart from our graph neural network model, we extract additional datasets, which represent each sample by a single feature vector. We consider three different feature sets: (1) For each sample, we aggregate the features of all flows for this sample using the previously used aggregation functions and concatenate the aggregates to a 318-dimensional feature vector. (2) To evaluate the importance of the graph structure for the baseline models, we extract a set of structural features from each graph: 2 global features (global clustering coefficient and assortativity) and 8 local node-features (degree, number of 2-hop neighbors, clustering coefficient, avg. neighbor degree, avg. neighbor clustering coefficient, number of edges in egonet, number of edges leaving egonet, betweenness centrality), which are aggregated over all nodes in the graph, again using the above aggregation functions, and concatenated, leading to a 40-dimensional feature vector. (3) To provide access to both types of features, we concatenate the flow and graph features to a combined 358-dimensional feature vector. Again, all constant feature columns have been removed. All feature matrices, including the edge feature matrices for our model, are standardized before training.

5.1 Supervised Malware Detection and Classification

We consider three supervised tasks, binary, category, and family classification. To ensure a fair and unbiased comparison, we follow a rigorous evaluation protocol. First, we split the dataset into a train, validation and test part. Each model is trained on the training set, hyper-parameters are chosen based on validation set performance using a grid search and results are reported on the test set using the optimal hyper-parameter values. All experiments are repeated on 30 randomly generated splits and mean and standard deviation of the results are reported. To ensure a balanced training set, we sample 100, 25 and 5 samples per class for training for binary, category and family classification, respectively.

	SVM-LIN	SVM-RBF	KNN	DT	RF	ADA	MLP	NF-GNN-CLF
Binary	98.29 ± 0.40	97.95 ± 0.32	98.02 ± 0.49	96.50 ± 0.85	97.93 ± 0.41	98.22 ± 0.94	98.60 ± 0.53	99.42 ± 0.45
Category	86.19 ± 0.92	89.81 ± 1.05	90.25 ± 1.10	86.81 ± 2.17	92.45 ± 0.72	82.52 ± 2.18	92.14 ± 1.32	95.45 ± 1.54
Family	59.92 ± 16.57	75.29 ± 10.14	75.01 ± 12.22	76.03 ± 26.73	87.19 ± 5.32	80.02 ± 22.32	75.60 ± 10.65	91.92 ± 6.00

Table 1: Weighted F1 scores for the three supervised tasks in terms of mean and standard deviation over 30 independent data splits.

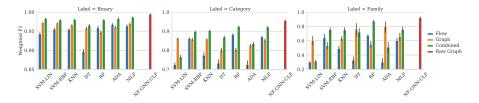


Fig. 2: Weighted F1 scores for the three supervised tasks using different feature sets. Results are reported over 30 independent data splits.

For binary and category classification, 5% of the remaining samples are sampled in a stratified fashion for validation, the remaining samples are used for testing. For family prediction, 20% of the non-training samples are chosen for validation to account for smaller class sizes. Stratification ensures that smaller classes are represented appropriately in the validation set. Again, to account for class imbalance, we report weighted F1 scores. In all considered settings, we checked that our models outperform the respective best competitor with statistical significance at P < 1e - 5 according to a Wilcoxon signed-rank test. We compare against 7 baseline algorithms with different inductive bias, Support Vector Machine (SVM) with linear and RBF-kernel, k-Nearest Neighbor Classifier (KNN), Decision Tree (DT), Random Forest (RF), Adaboost (ADA) and a Multi-Layer Perceptron (MLP) with up to two dense layers and ReLU and softmax activations. For all neural network models, we use early stopping based on validation set performance using a patience of 20 epochs and a maximum of 1000 epochs. The default learning rate for all MLP-models is fixed as 1e-3. For our model, we additionally apply dropout regularization before each dense layer and on the propagation matrices. All considered hyper-parameter values for all models are provided in Appendix A. Since the original feature vectors are rather high-dimensional, we introduce an additional hyper-parameter for each baseline model indicating whether or not to perform Principle Component Analysis (PCA) as feature reduction before training where 95% of the variance in the data is retained.

Prediction results for all three tasks are reported in Table 1. For each baseline model, the best feature set has been chosen based on validation set performance. While some baselines perform notably weaker than others, we can observe that all baseline models still exceed the best results reported in [23], namely at most

	OC-SVM-LIN	OC-SVM-RBF	LOF	KDE	IF	MLP-AE	MLP-OC	NF-GNN-AE	NF-GNN-OC
Flow	57.17 ± 4.81	70.01 ± 1.90	73.15 ± 1.22	72.50 ± 1.03	70.39 ± 1.12	71.64 ± 1.20	81.29 ± 4.07		1
Graph	54.60 ± 19.32	67.19 ± 2.89	58.57 ± 5.12	91.79 ± 0.66	90.73 ± 1.31	89.56 ± 0.77	94.00 ± 1.32	95.34 ± 0.85	96.75 ± 1.22
Combined	58.21 ± 4.83	76.07 ± 1.78	77.94 ± 1.56	86.60 ± 1.07	85.73 ± 2.21	83.04 ± 0.78	94.03 ± 4.47		1

Table 2: AUROC scores for unsupervised malware detection in terms of mean and standard deviation over 30 independent data splits. Our models use the raw graphs as input instead of the features extracted for the baseline models.

88.30%, 49.90%, and 27.50% precision/recall for binary, category, and family classification, respectively, by a large margin, even under a rigorous evaluation setup and using small training sets. This supports the main motivation of our approach to detect and classify malware using network flow graphs. Additionally, our proposed model can further boost performance significantly compared to the baselines. In particular, we exceed the performance reported in [23] by more than 11%, 45% and 64%, respectively. Notably, all baselines except RF struggle with large variance in the results for family classification. To evaluate the importance of different feature sets for the baseline models, we compare individual performance in Figure 2. We can observe that almost all baseline models perform best on the combined flow and graph feature set. In most cases, the combination boosts performance significantly over the best individual feature set. Our model operating on the raw graphs still outperforms all baselines. An additional experiment investigating the influence of the number of layers on the performance of our model is provided in Appendix B.

5.2 Unsupervised Malware Detection

We further evaluate our approach in a more realistic unsupervised setting, where no labels are available for training. Our experimental setup is the same as in the supervised case with a few adjustments. To ensure a realistic distribution of benign and malicious samples, we perform stratified sampling to first split 20% of the samples for training and then 10% of the remaining samples for validation. The remaining samples are used for testing. All algorithms obtain access to the labeled validation set for hyper-parameter optimization but training is still unsupervised. We evaluate detection performance using AUROC since it inherently adjusts for class imbalance [7]. We evaluate against a set of popular baseline algorithms for anomaly detection, One-class SVM (OC-SVM) with linear and RBF-kernel, Local Outlier Factor (LOF), Kernel Density Estimation (KDE), Isolation Forest (IF), Autoencoder with dense layers (MLP-AE) and One-Class Neural Network with dense layers (MLP-OC). Again, all considered hyper-parameter values are provided in the supplement.

Table 2 shows the detection results for different feature sets. We can observe that several models report better prediction performance using only structural graph features. Thus, compared to the supervised setting, it is even more im-

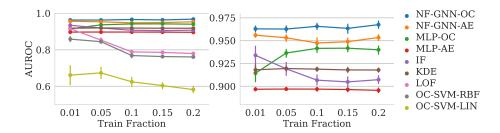


Fig. 3: AUROC scores for unsupervised malware detection using different fractions of training samples. The right-hand figure provides an enlarged view of the upper part of the left-hand figure.

portant to consider the structure of the network flow graph. While both neural network baselines as well as KDE and IF already exhibit high detection performance, our models can again boost performance by a significant margin, demonstrating the importance of learning suitable representations from network flow graphs. In practice, there is often a shortage of available training data, even of unlabeled data. Thus, we further investigate performance using different amounts of training data where we gradually reduce the fraction of training samples from 20% to 1%. For each training set size, a new grid search is performed to determine the best hyper-parameters for each model. Figure 3 shows that while some models perform worse with more available training data, possibly due to overfitting to anomalies in the training set, especially MLP-OC and NF-GNN-OC benefit from more training data. Over all training set sizes, both of our models consistently outperform all competitors.

6 Conclusion

We propose a novel network flow graph-based approach to malware detection and classification, where we monitor network traffic generated by a candidate application and extract a flow graph, which models communication between devices during the considered time frame. In addition, we propose 3 novel graph neural network models for supervised and unsupervised settings. Empirically, we found that even baseline models operating on manually extracted graph and flow features perform very well in all settings, exceeding previously reported results by a large margin. In addition, our proposed models automatically learn suitable representations of network flow graphs and are able to boost performance significantly further. Ablation studies examine the influence of different features sets, number of network layers and training set size on detection/classification performance. In future work, we plan to consider additional network architectures, such as attention, model temporal dynamics, and consider explainability of model decisions.

References

- Abuthawabeh, M.K., Mahmoud, K.: Enhanced android malware detection and family classification, using conversation-level network traffic features. IAJIT (2020)
- 2. Anderson, B., Quist, D., Neil, J., Storlie, C., Lane, T.: Graph-based malware detection using dynamic analysis. Journal in Computer Virology (2011)
- Battaglia, P.W., Hamrick, J.B., Bapst, V., Sanchez-Gonzalez, A., Zambaldi, V., Malinowski, M., Tacchetti, A., Raposo, D., Santoro, A., Faulkner, R., et al.: Relational inductive biases, deep learning, and graph networks. arXiv preprint arXiv:1806.01261 (2018)
- 4. Bazrafshan, Z., Hashemi, H., Fard, S.M.H., Hamzeh, A.: A survey on heuristic malware detection techniques. ICIKT (2013)
- Bekerman, D., Shapira, B., Rokach, L., Bar, A.: Unknown malware detection using network traffic classification. CNS (2015)
- Bronstein, M.M., Bruna, J., LeCun, Y., Szlam, A., Vandergheynst, P.: Geometric deep learning: going beyond euclidean data. SPM (2017)
- Campos, G.O., Zimek, A., Sander, J., Campello, R.J., Micenková, B., Schubert, E., Assent, I., Houle, M.E.: On the evaluation of unsupervised outlier detection: measures, datasets, and an empirical study (2016)
- 8. Cen, K., Shen, H., Gao, J., Cao, Q., Xu, B., Cheng, X.: Anae: Learning node context representation for attributed network embedding. arXiv preprint arXiv:1906.08745 (2020)
- Chalapathy, R., Chawla, S.: Deep learning for anomaly detection: A survey. arXiv preprint arXiv:1901.03407 (2019)
- 10. Draper-Gil, G., Lashkari, A.H., Mamun, M.S.I., Ghorbani, A.A.: Characterization of encrypted and vpn traffic using time-related features. ICISSP (2016)
- 11. Faruki, P., Laxmi, V., Gaur, M.S., Vinod, P.: Mining control flow graph as api call-grams to detect portable executable malware. SIN (2012)
- Gibert, D., Mateu, C., Planes, J.: The rise of machine learning for detection and classification of malware: Research developments, trends and challenges. JNCA (2020)
- 13. Gilmer, J., Schoenholz, S.S., Riley, P.F., Vinyals, O., Dahl, G.E.: Neural message passing for quantum chemistry. ICML (2017)
- 14. Gong, L., Cheng, Q.: Exploiting edge features for graph neural networks (2019)
- Hassen, M., Chan, P.K.: Scalable function call graph-based malware classification. CODASPY (2017)
- He, K., Zhang, X., Ren, S., Sun, J.: Deep residual learning for image recognition. CVPR (2016)
- 17. Jiang, H., Turki, T., Wang, J.T.: Dlgraph: Malware detection using deep learning and graph embedding. ICMLA (2018)
- 18. Jiang, X., Zhu, R., Li, S., Ji, P.: Co-embedding of nodes and edges with graph neural networks. TPAMI (2020)
- 19. John, T.S., Thomas, T., Emmanuel, S.: Graph convolutional networks for android malware detection with system call graphs. ISEA-ISAP (2020)
- 20. Kinable, J., Kostakis, O.: Malware classification based on call graph clustering. Journal in computer virology (2011)
- 21. Kipf, T., Fetaya, E., Wang, K.C., Welling, M., Zemel, R.: Neural relational inference for interacting systems. ICML (2018)
- 22. Kipf, T.N., Welling, M.: Semi-supervised classification with graph convolutional networks. ICLR (2016)

- 23. Lashkari, A.H., Kadir, A.F.A., Taheri, L., Ghorbani, A.A.: Toward developing a systematic approach to generate benchmark android malware datasets and classification. ICCST (2018)
- Lin, L., Wang, H.: Graph attention networks over edge content-based channels. KDD (2020)
- Muna, A.H., Moustafa, N., Sitnikova, E.: Identification of malicious activities in industrial internet of things based on deep learning models. JISA (2018)
- Prasse, P., Machlica, L., Pevný, T., Havelka, J., Scheffer, T.: Malware detection by analysing network traffic with neural networks. SPW (2017)
- 27. Ruff, L., Vandermeulen, R., Goernitz, N., Deecke, L., Siddiqui, S.A., Binder, A., Müller, E., Kloft, M.: Deep one-class classification. ICML (2018)
- Schlichtkrull, M., Kipf, T.N., Bloem, P., Van Den Berg, R., Titov, I., Welling, M.: Modeling relational data with graph convolutional networks. ESWC (2018)
- Shang, C., Liu, Q., Chen, K.S., Sun, J., Lu, J., Yi, J., Bi, J.: Edge attention-based multi-relational graph convolutional networks. arXiv preprint arXiv:1802.04944 (2018)
- Simonovsky, M., Komodakis, N.: Dynamic edge-conditioned filters in convolutional neural networks on graphs. CVPR (2017)
- 31. Taheri, L., Kadir, A.F.A., Lashkari, A.H.: Extensible android malware detection and family classification using network-flows and api-calls. ICCST (2019)
- 32. Tax, D.M., Duin, R.P.: Support vector data description. Machine learning (2004)
- 33. Wu, Z., Pan, S., Chen, F., Long, G., Zhang, C., Philip, S.Y.: A comprehensive survey on graph neural networks. TNNLS (2020)
- 34. Xu, K., Li, C., Tian, Y., Sonobe, T., Kawarabayashi, K.i., Jegelka, S.: Representation learning on graphs with jumping knowledge networks. ICML (2018)
- 35. Zhang, X., Xu, C., Tian, X., Tao, D.: Graph edge convolutional neural networks for skeleton based action recognition. TNNLS (2019)

A Hyper-Parameter Optimization

For the sake of a fair comparison, hyper-parameters of all models are optimized by a grid search based on performance on a separate validation set. For each algorithm, we consider a set of possible values for each of its adjustable hyper-parameters. While some common choices can be found in the literature, for the remaining hyper-parameters we determine potential values, which seem most promising within the available computational budget. The considered hyper-parameter values for all supervised models can be found in Table 3, the values considered for the unsupervised models are provided in Table 4.

B Influence of the Number of Message Passing Layers

To further evaluate the influence of the number of layers on the performance of our model, we compare different choices for the supervised classification tasks in Figure 4. We can observe that modeling 2-hop interactions between endpoints can boost performance on the binary prediction tasks, while direct interactions are more important for the remaining two tasks. In general, performance remains rather stable for different numbers of layers.

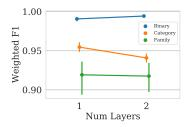


Fig. 4: Performance of our model on supervised tasks with different numbers of layers.

Algorithm	Parameter	Values
Support Vector Machine (SVM)	C	$[2^{-7}, 2^{-6}, \dots, 2^7]$
	γ (RBF-kernel)	$[2^{-7}, 2^{-6}, \dots, 2^7]$
k-Nearest Neighbor Classifier (KNN)	num. neighbors	[1, 2, 3, 5, 8, 13, 21]
Decision Tree (DT)	max. depth	[2,5,10,None]
	max. features	[sqrt,None]
Random Forest (RF)	num. estimators	[10, 100, 1000]
	criterion	[entropy,gini]
	max. features	[sqrt,None]
Adaboost (ADA)	num. estimators	[10, 100, 1000]
	learning rate	[1e-3, 1e-2, 1e-1, 1]
Multi-Layer Perceptron (MLP)	num. layers	[1,2]
	num. hidden	[16, 32, 64, 128]
	L2-reg.	[0, 1e-1, 1e-2, 1e-3, 1e-4]
NF-GNN-CLF (ours)	num. layers	[1,2]
	num. hidden	[16, 32, 64, 128]
	learning rate	[1e-3, 1e-2]
	dropout prob.	[0, 0.2, 0.4, 0.6]
	pool	[mean,add,max]

Table 3: Hyper-parameter values used in grid search for supervised algorithms.

Algorithm	Parameter	Values
One-class SVM (OC-SVM)	ν	[1e-2, 1e-1]
	γ	$[2^{-10}, 2^{-9}, \dots, 2^{10}]$
Local Outlier Factor (LOF)	num. neighbors	[1, 2, 3, 5, 8, 13, 21]
Kernel Density Estimation (KDE)	bandwidth	$[2^{0.5}, 2, \dots, 2^5]$
Isolation Forest (IF)	num. estimators	[10, 100, 1000]
	max. features	[256,None]
Autoencoder (MLP-AE)	num. layers	[1,2]
	num. hidden	[16, 32, 64, 128]
	L2-reg.	[0, 1e-1, 1e-2, 1e-3, 1e-4]
One-class MLP (MLP-OC)	num. layers	[1,2]
	num. hidden	[16, 32, 64, 128]
	L2-reg.	[0, 1e-1, 1e-2, 1e-3, 1e-4]
NF-GNN-AE (ours)	num. layers	[1,2]
	num. hidden	[16, 32, 64, 128]
	learning rate	[1e-3, 1e-2]
	dropout prob.	[0, 0.2, 0.4, 0.6]
	pool	[mean,add,max]
NF-GNN-OC (ours)	num. layers	[1,2]
	num. hidden	[16, 32, 64, 128]
	learning rate	[1e-3, 1e-2]
	dropout prob.	[0, 0.2, 0.4, 0.6]
	pool	$\left[mean, add, max \right]$

 ${\it Table 4: Hyper-parameter\ values\ used\ in\ grid\ search\ for\ unsupervised\ algorithms.}$